

Using digital repeat photography for monitoring the regrowth of a clear-cut area



Photo: INES, Lund University

Ludvig Forslund

2014
Department of
Physical Geography and Ecosystems Science
Lund University
Sölvegatan 12
S-223 62 Lund
Sweden



Using digital repeat photography for monitoring the regrowth of a clear-cut area

Ludvig Forslund

Bachelor degree thesis 15 credits in *Physical Geography and Ecosystem Science*

Supervisor: Harry Lankreijer

Technical supervisors: Patrik Vestin,
Lars Eklundh & Hongxiao Jin

Course coordinator: Jonas Ardö

Department of Physical Geography and Ecosystems Science

Lund University

2014

Abstract

The use of inexpensive digital cameras in phenological research has been acclaimed since results in previous research have shown that they are reliable and precise in measuring greenness of vegetation. The work of this thesis aims to broaden the applicability by studying how well the method performs when measuring the regrowth of a clear-cut area. This is needed to complement existing research that primarily uses the technique to study phenology. Data acquisition from the digital images was carried out with the use of chromatic coordinates in comparison to parallel measurements of sensor-based NDVI. These time series were analyzed through correlations, measuring the linear dependency and covariance. The results show significant similarities between the two measured time series and the increase in vegetation denseness during the studied period (2011-2013). It is also shown that the chromatic coordinates are more sensitive to variations in chlorophyll greenness than NDVI.

These results, together with previous research, show that the digital camera is a valuable tool that is possible to apply to forest research and industry. Studies of clear-cut areas have shown that soil carbon release is strongly dependent on initial vegetation, a relationship that is possible to study following the results of this thesis. However, more research is needed to calibrate the method for measurements in different forest types and climate zones, before this is reality. The use of ground-level reference panels are also analyzed but fails to provide the reliable information needed. Too many sources of error are detected where the brightness calibration does more harm than good. Instead, chromatic coordinates and smoothing of the time series are used for suppressing the diurnal and seasonal variations in scene illumination.

Keywords: *Chromatic coordinates, clear-cut, digital images, NDVI, near-surface remote sensing, Norunda, PhenoCam, scene illumination*

Sammanfattning

Digitala övervakningskameror har tidigare använts inom fenologisk forskning för att kunna mäta grönskan i trädkronor. Man har under en längre tid kunnat koppla lövträdets årscykel till klimatförändringar och på så sätt haft ett starkt incitament att studera sambandet. I denna uppsats utforskas möjligheten att applicera metoden med digitalkameror på ett nyligen kalhugget område för att se om man kan mäta återväxten under tre års tid (2011-2013). Genom att extrahera pixelvärden och beräkna grönskan kan man under de tre växtsäsongerna studera en signifikant ökning i markvegetation. Under arbetet har digitalkamerorna jämförts med sensordata, så kallad NDVI, för att studera huruvida metoden kan mäta sig med mer precis och konventionell teknik. Detta har den visat sig kunna där de digitala kamerorna, i vissa fall, visat sig vara mer känsliga för hastiga variationer i grönska än de parallella sensormätningarna.

Forskning har bevisat att det största läckaget av markbundet kol sker under de inledande åren efter skogsfällning. Detta kol har skogens jordar tidigare förvarat och konserverat, men efter fällning läcker det ut i atmosfären som koldioxid. Läckaget har också visat sig ha ett starkt samband med den initiala återväxten av markvegetation på kalhygget. Digitalkamerorna skulle således kunna användas för att studera relationen. I denna uppsats diskuteras därför vidare användning av metoden inom skogsforskning och industri. En annan applicering, i form av vegetationsövervakning, undersöks också i denna uppsats där digitalkamerorna skulle kunna vara till stor hjälp inom skogsindustri och skogsvård. Målet med denna uppsats har alltså varit att utforska användningen av digitala kameror för att studera möjligheten att övervaka återväxten av ett kalhygge.

Nyckelord: *Kromatiska koordinater, kalhygge, digitala bilder, NDVI, Norunda, fjärranalys, PhenoCam, bildljusstyrka*

Acknowledgements

I would like to thank my supervisor Harry Lankreijer for giving me valuable insights and guidance through this thesis. I would also like to extend my gratitude to Patrik Vestin for helping me with data collection and technical supervision, as well as Lars Eklundh and Hongxiao Jin for theoretical and practical guidance.

Table of contents

Abstract	i
Sammanfattning	ii
Acknowledgements	iii
1. INTRODUCTION	1
1.1 Aim and Objectives	2
1.2 Theoretical Background	2
1.2.1 Extraction of greenness	2
1.2.2 NDVI	3
1.3 Past Research	3
2. MATERIALS	5
2.1 Study area	5
2.2 Data Description	5
2.2.1 Camera pictures (RGB)	5
2.2.2 NDVI	5
3. METHODOLOGY	7
3.1 Camera pictures (RGB)	7
3.2 NDVI	8
3.3 Scene illumination and brightness	9
3.4 Statistics	10
3.4.1 Data Arrangement	10
3.4.2 Linear correlation	10
3.4.3 Autocorrelation	11
3.4.4 Spearman ranked correlation	11
4. RESULTS	13
4.1 Time Series	13
4.2 Statistics	14
4.2.1 GCC-NDVI comparison	14
4.2.2 Autocorrelation and Spearman	15
4.3 Illumination calibration	16
5. DISCUSSION	17
5.1 Relationship between GCC and NDVI	17
5.2 Scene Illumination	18
5.2.1 Reference panels	18
5.3 Applicability	19
5.3.1 Scientific	19
5.3.2 Industrial	19
5.3.3 Future research	19
6. CONCLUSION	21
REFERENCES	22

1. INTRODUCTION

Digital repeat photography was first elaborated by Richardson et al. (2007) as a promising method for studying the annual cycle of deciduous vegetation i.e. phenology. Earlier, measurements were carried out through field observations done by individuals with the appropriate knowledge (Richardson et al. 2007). Phenology has also been studied during the last 20 years through satellite remote sensing (Hufkens et al. 2012); a tool that is able to analyze considerable larger regions than its counterpart, field observations. On the other hand, satellite measurements are more imprecise and measures on a larger, coarser scale (Hufkens et al. 2012). As one can see, there is conflict between scale and precision in the phenological research methodology.

When the digital technology of photography was getting more sophisticated, during the middle part of the past decade, Richardson et al. (2007) started to see the opportunities with such an objective and quantifiable tool. Since research in phenology is linked to climate change (Morissette et al. 2009), the tool is believed to have a significant importance within this scientific field. These circumstances resulted in a development of a modern method, using digital cameras, which got the attention of some scientists around the world (Ahrends et al. 2008; Richardson et al. 2007).

The goal with this thesis is to examine if digital cameras can be used to deliver equally reliable vegetation data as other conventional methods like sensor-based NDVI. The aim is set to find similar results to that of past research by Ahrends et al. (2009); Migliavacca et al. (2011) and Richardson et al. (2009), when used on a clear-cut. This will be achieved by studying the relationship between digital images and NDVI measurements from a clear-cut area in Norunda forest situated in central Sweden close to Uppsala. The camera at Norunda aims to capture the regrowth of the initially bare ground, instead of focusing on canopies. If this method proves its reliability it could possibly broaden the applicability of digital repeat photography. Sectors such as the forest industry and research may benefit if this is the case. The method is an inexpensive tool, compared to satellite and field observations, as it uses standard commercial cameras where it also has shown to be precise and reliable despite its simplicity (Richardson et al. 2007; 2009). The main advantage according to Richardson et al. (2007) is that the digital repeat photography is a hybrid between the more traditional field observations and the radiometric sensors mounted on towers, planes or satellites. The digital images can hence be interpreted by a human eye alongside the calculations and quantifications. This makes it possible to check abnormalities found in the data by examining the picture archive and identify the source of error (Richardson et al. 2007), a procedure that is not possible with radiometric measurements, where speculation is often the only approach.

The method is still in an early stage and needs to be further investigated to see whether there are other suitable applications. This thesis will give further input to earlier research by applying the method on a clear-cut, instead of tree canopies.

1.1 Aim and Objectives

This thesis is set to expand the use of digital repeat photography by exploring the applicability on other areas and past research. This will be investigated through the following questions:

- 1) Is the method of digital photography sufficient for monitoring the sparse vegetation on a clear-cut area?
- 2) Are there other scientific areas possible with the results of this thesis?
- 3) What is the most appropriate method for suppressing scene illumination variation?

1.2 Theoretical Background

1.2.1 Extraction of greenness

The way of using digital photography as a tool for remote sensing was initially thought out by Richardson et al. (2007), who elaborated a method intended to track phenological patterns with digital webcam images. The main theory is to extract greenness information from digital images by measuring the Red, Green and Blue (RGB) channels of every pixel. Each channel contains a Digital Number (DN) with a value between 0-255 which defines the brightness of respective color. These pixel-values are then measured and extracted from a user defined Region Of Interest (ROI) that limits which pixels to include in the measurement (Sonnentag et al. 2012). The total pixel values are then averaged and returned as the mean RGB of the ROI (Richardson et al. 2009). To further extract the greenness information from the average RGB two formulas, *Excess Green (ExG)* and *Green Chromatic Coordinates (GCC)*, are possible to apply:

$$ExG = 2 * Green - (Red + Blue) \quad (1)$$

$$GCC = \frac{Green}{(Red+Green+Blue)} \quad (2)$$

where the colors (Red, Green, Blue) are the mean values of the ROI and represented in digital numbers (Richardson et al. 2009).

The GCC output is an index ranging between 0 and 1 where ExG is ranging between 0 and 510 but can easily be converted to a 0-1 index as well. According to Sonnentag et al. (2012) the GCC is also a superior method, compared to ExG, because of its ability to suppress diurnal and weather-related effects on scene illumination. These are caused by differences in cloud cover and sun altitude, which gives each picture its unique scene illumination. These variations will affect the color sampling which needs to be normalized in order for the pictures to be comparable. Sonnentag et al. (2012) suggest the use of chromatic coordinates (GCC) and to further eliminate the diurnal and seasonal changes in scene illumination, a three-day smoothing is recommended. This is calculated using a moving window, where the 90th percentile of all GCC values within three days are averaged to the center day (Sonnentag et al. 2012). The use of green chromatic coordinates is necessary for looking at the relative brightness of the green color compared to the red and blue (Sonnentag et al. 2012).

Another method to eliminate the diurnal and seasonal variations in scene illumination is the use of reference panels. These are used as a neutral and perpetual reference in each picture not dependent on anything except the incoming light. By placing a ROI on the reference panel the RGB values can be extracted parallel to the vegetation GCC measurements (Sonnentag et al.

2012). A dilemma that has been discovered by Ahrends et al. (2008) is the choice of color of the reference panel. When it is too white it often gets oversaturated on sunny days. Because of this it is recommended to use a panel with a variety of gray colors instead (Richardson et al. 2009). Besides the choice of color, this method has another weakness, where the strong variation of the reference panel is imported to the GCC values (Sonnentag et al. 2012).

A question that is relevant for this thesis is whether the white balance of the camera should be fixed or automatic. According to Richardson et al. (2009) the fixed setting reduces the day-to-day variability and thus suppresses the diurnal variation. However, Zhao et al. (2012) concludes the opposite by measuring two cameras, with different white balance settings, without a significant divergence.

1.2.2 NDVI

The Normalized Difference Vegetation index (NDVI) is widely used in monitoring of vegetation. The sensor measuring NDVI can be mounted on satellites, airplanes and towers (far, near and very near remote sensing), depending on the target information (Lillesand et al. 2008). For this thesis the tower-mounted version of NDVI sensors was used, although the theoretical work is similar on all platforms. The raw output from the two channels of the sensor is given in millivolt (mV) where one channel measures the Near Infrared Radiation (NIR) (central wavelength= 860 nm) and the other Red visible light (central wavelength= 650 nm) (Eklundh et al. 2011). To construct the NDVI index the electrical data is transformed into Ratio Vegetation Index (RVI) through:

$$RVI = \frac{\bar{\rho}_{NIR}}{\bar{\rho}_{Red}} \quad (3)$$

where $\bar{\rho}$ is the average footprint reflection (nm) for each channel ($\bar{\rho}_{Red}$, $\bar{\rho}_{NIR}$) calculated with:

$$\bar{\rho} = \frac{\pi \bar{L}_r}{E} \quad (4)$$

where differences in diurnal variations are calibrated. This is achieved by using an upward-looking sensor measuring the hemispherical irradiance (E) [$\mu\text{mol} \cdot \text{s}^{-1} \cdot \text{m}^{-2}$]. The mean footprint reflectance of the down-looking sensor (\bar{L}_r) [$\mu\text{mol} \cdot \text{s}^{-1} \cdot \text{m}^{-2} \cdot \text{sr}^{-1}$] is adjusted so that errors, caused by the off-nadir perspective of the sensor, are normalized (Eklundh et al. 2011).

1.3 Past Research

Earlier work within the field has been revolving around the work of Andrew D. Richardson who has developed the method for RGB-camera greenness analysis. The aim of past research has been to monitor the spatial and temporal variation in canopy phenology (Richardson et al. 2009), which earlier has been studied through field observations (Richardson et al. 2007).

Richardson et al. (2007) argue for a methodological improvement of phenology research. The main purpose is to establish a cheaper, more objective and superior method for this kind of analysis. The main problem with the field observations is that they are too labor-intensive and imprecise, where observer bias makes it discontinuous and hard to quantify (Richardson et al. 2007). Richardson et al. (2007) instead finds the digital photography method to be well suited for this task and discuss the advantages with the possibility of a large scale data gathering across the USA, which is feasible because of the low cost, straightforward technology that is manageable by almost anybody. For this thesis the method elaboration of Richardson et al. (2007) is the scientific foundation.

The method development by Richardson et al. (2007) includes a study of camera types for monitoring greenness shifts. The study investigates the most appropriate cameras and usage when it comes to analyzing outdoor environments. The aim is to find a camera that represents the study area without any additional layers or settings affecting the objectiveness of the pictures. This should be fulfilled to a reasonable price able to compete with the other technologies in the field, such as sensors (Richardson et al. 2009). To analyze the pictures, a script was constructed intended to gather the RGB information from each picture (Richardson et al. 2007). A study of different methods for analyzing greenness is included in the 2007 article where *Excess Green (ExG)* and *Green Chromatic Coordinates (GCC)* are constructed. Richardson concludes the 2007 article by comparing the digital camera method to field observations and radiometric approaches. The main disadvantage according to Richardson et al. (2007) is the complications with the variability in normalized channel brightness. A downside that is improved by Sonnentag et al. (2012) with further research on smoothed chromatic coordinates. An advantage is that digital cameras already exist on many places, as crime prevention etc., where the recorded pictures with vegetation can be used for large scale studies (Richardson et al. 2007).

Moving a year ahead Hella E. Ahrends published an article that deals with a similar research to Richardson et al. (2007) where it is investigated whether digital photography is a reliable method for monitoring phenology. Ahrends et al. (2008) also studies the possibility of measuring phenological information at species level as a precision analysis. The article also recognizes the difficulties with scene illumination and problematizes the use of reference panels (Ahrends et al. 2008). As Richardson et al. (2007), Ahrends et al. (2008) also stress the applicability of larger scale analysis for future research. However, Ide and Oguma (2010) add that a technical protocol is needed for this to be possible, a protocol which determines whether fixed white balance should be used or not, color calibration, file format and resolution. Ahrends et al. (2009) also successfully link measurements of GCC and Gross Primary Production (GPP) derived from CO₂ flux.

The second major part in the research of digital repeat photography is the work of Sonnentag et al. (2012). In this article the emphasis lies on studying and evolving the methodology, especially within the seasonal and diurnal changes in scene illumination. This is a problem Ahrends et al. (2009) and Richardson et al. (2009) address as having a major impact on the uncertainty analysis. Migliavacca et al. (2011) initially starts to propagate for the use of chromatic coordinates which Sonnentag et al. (2012) investigates in more depth. As described earlier, Sonnentag et al. (2012) find it more reliable with the use of smoothed chromatic coordinates than to calibrate with reference panels. Sonnentag et al. (2012) also demonstrates that the calculated GCC result of digital repeat photography is not just seasonal changes in incoming solar radiation. When measuring GCC of a vegetation free area (desert), the results show no seasonal variation. This is an outcome that indicates on a very small influence of scene illumination and thus a correlation of vegetation denseness and GCC seasonality (Sonnentag et al. 2012).

Hufkens et al. (2012) later studies the link between digital repeat photography and satellite data, a more traditional instrument for measuring phenology. The article seeks to find out whether the ground based measurements can be used to validate the satellite images, an effort to scale up the use digital repeat photography to regional and even continental levels. Hufkens et al. (2012) conclude that a formal protocol for evaluation and calibration is needed, a similar statement like that of Ide and Oguma (2010).

2. MATERIALS

2.1 Study area

The study area is limited to a 270 x 250 meters large clear-cut area in Norunda (Lat: 60.086516, Lon: 17.468792) 30 kilometers northwest of Uppsala, Sweden. The trees in the area were felled mid-2009 where measurements such as NDVI, gas fluxes and camera pictures started in 2010. The site is situated in a humid continental climate (Dfb according to the Köppen classification), or ENF in the IGBP ecosystem classification. The Mean Annual Precipitation is 527 mm and the Mean Annual Temperature is 5.5 °C (Lundin et al. 1999).

2.2 Data Description

2.2.1 Camera pictures (RGB)

The primary data for this thesis was acquired using a Mobotix M24M-Sec monitoring camera taking pictures every hour between 7 A.M and 16 P.M, from 2010 to 2013. The camera is mounted 25 m above the ground on a telescopic mast (Figure 1) overlooking the western part of the clear-cut. The output consisted of the Joint Photographic Experts Group (JPEG)-files with 2048 x 1536 pixels and a 96 dpi resolution, where every pixel contains the 24 bit-depth RGB information. The digital RGB code consists of a value for each color reaching from 0 to 255 where [R G B] = [0 0 0] is black, [R G B] = [255 255 255] is white, and everything in-between is a mixture of color tones.

Some corrections were necessary to consider due to disturbances such as a lens change from wide (Mobotix L22; 90°) to narrow (Mobotix L32; 60°) angle on June 21 2011. The other disturbance is a setting configuration changing the white balance of the camera from automatic/relative to a fixed irradiance temperature at 7000 °K the July 1 2013. Also, because of diurnal changes in scene illumination, some manual removal of pictures was necessary to make since only midday pictures (11:00 – 13:00) were used (Ahrends et al. 2008). Also pictures with disorders such as a water covered lens and snow cover were removed. The above exclusion resulted in a reduction of pictures for analysis from 8650 to 1727. However, the major part of the excluded pictures was morning and afternoon images, as well as the whole winter season. Pictures with snow cover and water on the lens only accounted for a handful of the total.

Late August 2011 a black and white reference panel is placed on the ground in the center of the picture (Figure 2). This is destined to be used as a calibration for variations in incoming solar radiation, where the panel works as a reference inside each picture. This is more thoroughly described in the methodology section.

2.2.2 NDVI

The NDVI time series consists of data reaching from May - October 2011 - 2013. The SKYE 2-channel sensor is mounted just above the camera at 25.8 meters with a western heading and a 40° angle off-nadir. The Field-of-View (FOV) is set to 25°

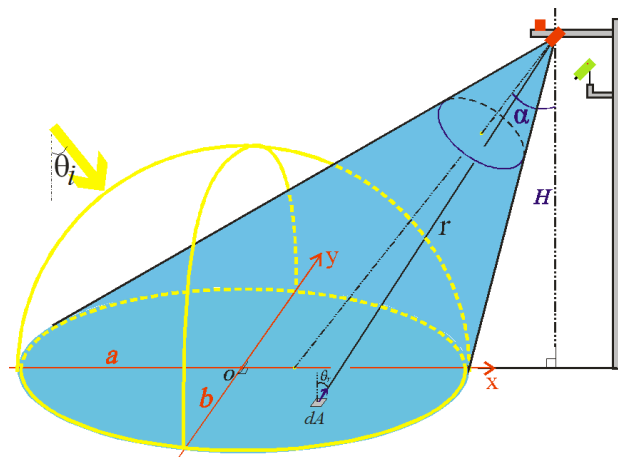


Figure 1: Geometry diagram of the sensors (Red), mounted at height H (25.8 m) and with the ellipse-shaped footprint where $a = 9.8$ m and $b = 7.4$ m. Digital camera (Green) at height (25 m) (Source: Eklundh et al. (2011); modified by the author)

which results in an ellipse-shaped, ground level footprint with an area of $\sim 226 \text{ m}^2$ (Figure 1). The sensor measuring the hemispherical irradiance is mounted at the same height and 0° off-zenith (Figure 1).

The data was received in the RVI format that had gone through the earlier described transformation (Section 1.2.2), performed by Eklundh et al. (2011), and is transformed into NDVI through:

$$NDVI = \frac{NIR-Red}{NIR+Red} = \frac{\frac{NIR}{Red}-1}{\frac{NIR}{Red}+1} \xrightarrow{\text{(Equation 3)}} \frac{RVI-1}{RVI+1} \quad (5)$$

(Jin Personal communications, 2013). NDVI values range between -1 and +1, where NDVI below zero represents water and snow and NDVI above zero represents vegetation concentration (Weier and Herring 2000). Water and snow absorbs the Near Infrared Radiation (NIR) and emit red radiation thus give a negative NDVI (see equation 5). On the other hand vegetation absorbs red radiation and reflects NIR radiation thus a positive NDVI. NIR is reflected off the cell structure from healthy leaves, so the more leaves a plant or ecosystem produce, the more reflected NIR.

3. METHODOLOGY

3.1 Camera pictures (RGB)

The RGB-data from each picture was extracted using the PhenologyCam Image processor v1.2 written by Hufkens (2010), with some changes made exclusively for this study. The program is constructed as a MATLAB (R2013a; Mathworks, Natick, Massachusetts, USA) script and its main function is to evaluate the average RGB-levels inside a user defined Region of interest (ROI). The ROI seen in figure 2 is first and foremost defined by the NDVI footprint, which is a necessity for later comparison between the two measurements. The distortion

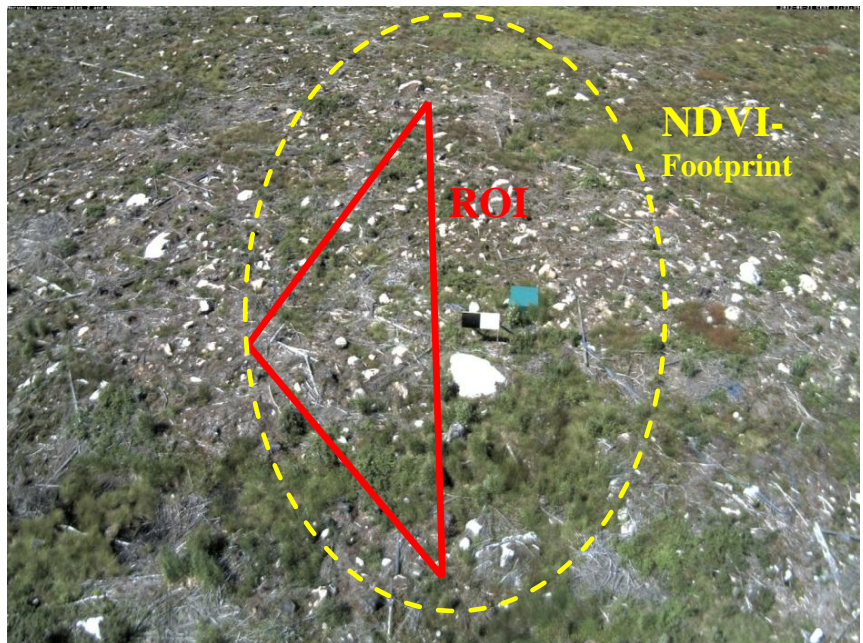


Figure 2: One of the many pictures from Norunda with the defined and used ROI (Region Of Interest) inside the calculated NDVI-Footprint.

(Figure 2) along the edges of the pictures is also taken into account when defining the ROI. Other factors considered, are the large stone and reference panels which are avoided due to the oversaturation on sunny days (more thoroughly explained in later chapters). The three coordinates defining the ROI had to be calculated to fit within the NDVI-footprint, thus a small amount of points were preferred. However, the size of the ROI is the most important aspect to consider, where the more pixels the better analysis.

The gathered data consisted of one mean value per color channel of the ROI, which means three values per picture. These were calculated into GCC according to equation 2, and smoothed as described in the theoretical background section.

Winter season (November – March) was purposely removed from the time series due to risk of snow cover. There was no built in process within the GCC method that could distinguish between snow, water or vegetation. All of these reflected some kind of color which would automatically receive a GCC-value. White snow for example $[R\ G\ B] \approx [255\ 255\ 255]$ would get a GCC-value of ~ 0.33 (equation 2) or less. However, vegetation would always have a GCC above 0.33, where all non-vegetation would have values below 0.33. This means that snow covered pictures could be included without any harm, although problems with oversaturated snow would probably lead to disturbances and irregularities during wintertime. This was the reason they were excluded.

The fundamental difference between the GCC method and the NDVI is that the RGB-camera measures the reflected visible light and NDVI, as mentioned above, measures the NIR and Red visible light. Chlorophyll absorbs all visible light, except wavelengths within the $\sim 500 - 570\ nm$ spectral range, which is the region the human eye and brain defines as green light. To clarify, the GCC is an index of chlorophyll concentration within the ROI

(Figure 2) and the NDVI is an index of healthy leaf material and chlorophyll concentration within the footprint (Figures 1 & 2).

Due to the change in camera white balance on the 1st of July 2013, the subsequent data until the 1st of August deviates significantly (Figure 3). However, the data returns to the trend after the 1st of August, which makes it possible to perform an interpolation. This was achieved using a fitted trend function for 2013, where the faulty values were recalculated as equation 6 shows. To each interpolated value a random number within the standard deviation was added (equation 6). The standard deviation was calculated from 2013 values except the ones between the 1st of July and the 1st of August. If the standard deviation was not added to the function, the interpolated values would not be representable with the rest of the time series.

$$\text{Interpolated GCC}(x) = \text{trend}(x) + \text{Random}(-1:1) * \text{st.dev} \quad (6)$$

For the reason of making it easier to illustrate, the unsmoothed GCC values were used for the plots in figure 3. However, the same interpolation was performed on the smoothed GCC time series.

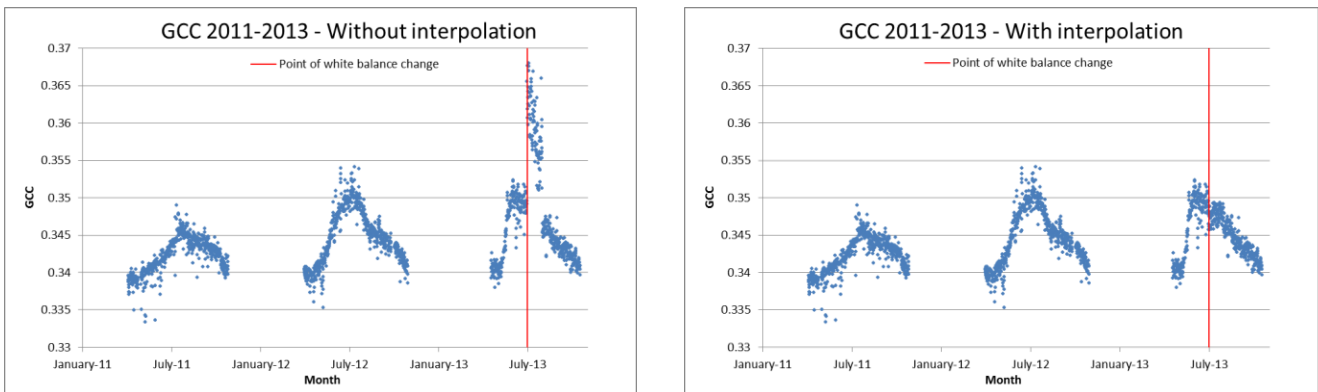


Figure 3: Comparison between with (right) or without (left) interpolation of GCC values between 1 July and 1 August 2013.

3.2 NDVI

As described in the 2.2.2-section the RVI-data was received calibrated and ready for analysis and could be transformed to NDVI by using equations 3 and 5.

The NDVI ground level footprint (Figure 2) was calculated using a script written by Jin (Personal communications, 2013) which calculates the sample area of a SKYE 2-channel sensor from the three inputs: sensor height, Field-Of View (FOV) and off-nadir angle. This returns the spread of sample points around the FOV center inside the footprint. The footprint can then be implemented into the camera pictures by knowing different scale references in the digital images.

As described in the 2. *Materials* section the NDVI measures snow, ice and water in negative index values due to low reflectance of NIR wavelengths (Lillesand et al. 2008). These negative values had to be removed for a statistical comparison between GCC and NDVI to be possible. This was achieved through the arrangement of data, which is described in section 3.4.1, where the snow covered digital images were excluded prior to analysis, and thus excluding the NDVI measurements of the same date automatically.

3.3 Scene illumination and brightness

Because of differences in cloud cover and sun altitude each picture gets its unique brightness level and thus a different scene illumination (Figure 4). This will affect the color sampling and needs to be normalized in order for the pictures to be comparable.



Figure 4: Two pictures with an hour apart as an example of difference in scene illumination. Black and white reference panels can be seen slightly down to the left of the green box and above the white stone.

To handle the problem with scene illumination and diurnal changes in brightness levels, two different methods can be applied. The first method treats the problem before analysis, where each picture is manipulated into an average brightness. This requires a script where the mean brightness is calculated and changes every pixel in each picture so that the illumination differences are eliminated. The second method with smoothed green chromatic coordinates is described in the 1.2.1 section and is used throughout this thesis.

Probably the first method would give better results but requires substantial amount of time. Therefore the smoothed GCC method was used in this study. It produces less data which of course affects the reliability of the analysis, but on the other hand makes the RGB-data more normalized.

The use of reference panels was also implemented in the work of this thesis to analyze the utility. Although they are discouraged in earlier research by Sonnentag et al. (2012) and Hufkens et al. (2012), they are implemented simply because of their existence and the fact that they can strengthen the credibility of the research. Unfortunately the reference panels used in Norunda clear-cut are dyed white and black (Figure 4), where a gray alternative would be preferable (Ahrends et al. 2008). Two ROI_{ref} (black and white panel) were defined for extraction of reference-RGB data from 2012. The reason the 2012 season was selected was because of the absence of disturbances, such as lens and white balance change. These changes disrupt the time series and make it harder and more time consuming to work with. As with the vegetation analysis these RGB values were used to calculate the GCC_{ref} (Equation 2) for each reference surface. The aim of the method is to calculate a Reference Index (RI) and then calibrate each measurement according to equations (7) and (8):

$$RI(x) = GCC_{ref}(x) - \overline{GCC_{ref}} \quad (7)$$

$$Calibrated\ GCC(x) = GCC(x) - RI(x) \quad (8)$$

where RI adds when equation 7 is below zero (darker scene illumination than normal) and subtracts when equation 7 is above zero (brighter scene illumination than normal).

Because of the experiences of oversaturation in the work of Ahrends et al. (2008), it was necessary to examine the risk by taking the average of the RGB values of the white panel. If

the mean RGB value equals 255 it was interpreted as oversaturated. To clarify, $\overline{RGB} = 255$ is possible if and only if $RGB = [255 \ 255 \ 255]$.

3.4 Statistics

3.4.1 Data Arrangement

To be able to study the usefulness of GCC methodology it is necessary to have a reliable source for comparison, in this case NDVI. Statistical tests and methods are used to spot the differences and similarities between the two time series where three different correlation-methods are applied in this thesis.

First, the two variables, NDVI and GCC, needs to be arranged. The time series are of different length and inconsistent which makes it necessary to sort after the dates of the shortest variable (Figure 5). For this kind of analysis, this is essential where the target is to compare each corresponding variable. This is done by writing a script that checks the first date of the “Date (GCC)”-vector and then searches for a match in the “Date (NDVI)”-vector. When the program finds the corresponding date it returns the related NDVI-value and then proceeds to the next row. This is a necessary approach when the amounts of values are too many to arrange by hand.

DATE (GCC)	GCC	Date (NDVI)	NDVI
5-5-11	0.3393	5-5-11	0.3111
8-5-11	0.3400	6-5-11	0.1760
11-5-11	0.3410	7-5-11	0.1560
14-5-11	0.3405	8-5-11	0.1663
17-5-11	0.3403	9-5-11	0.1638
		10-5-11	0.1659
		11-5-11	0.1659
		12-5-11	0.1833
		13-5-11	0.18676
		14-5-11	0.20083
		15-5-11	0.3848
		16-5-11	0.25897
		17-5-11	0.21076

DATE	GCC	NDVI
5-5-11	0.3393	0.3111
8-5-11	0.3400	0.1663
11-5-11	0.3410	0.1659
14-5-11	0.3405	0.2008
17-5-11	0.3403	0.2108

Figure 5: Arrangement of data in order to fit. Bold numbers are selected from each column where GCC dates are the reference. These numbers are just a fraction of the total amount.

3.4.2 Linear correlation

With the arranged data it was possible to calculate the Pearson correlation coefficient accordingly:

$$r = \frac{\text{covariance}(GCC, NDVI)}{\sigma_{GCC} * \sigma_{NDVI}} \quad (9)$$

and with the coefficient, the significance of the correlation can be calculated through the t distribution:

$$t = \frac{r\sqrt{n-2}}{\sqrt{1-r^2}} \quad (10)$$

where σ_{GCC} and σ_{NDVI} represents the standard deviation of the population for respective variable, and where n is the sample size (Matematikcentrum 2012).

3.4.3 Autocorrelation

When studying time series, it is highly relevant to look for time-dependence in the observed variables GCC and NDVI to ensure that the perceived trend distinguishes itself from white noise. Time-dependence of time series can be found by computing the autocorrelation. This can be described as calculating r (Equation 9) between values at different time intervals i.e. lags (Figure 6). If there is a significant correlation at lag distance k there is time-dependence between values that are k -lags apart. For example if a significant correlation is found at lag distance $k = 2$ throughout the time series, there is a time-dependence in-between two measurements (Figure 6) (Matematikcentrum 2012).

This thesis looks for dependence over time t i.e. seasonality, which is why an autocorrelation is implemented. The correlation coefficient ρ_k at each lag k is achieved accordingly:

$$\rho_k = r_k = \frac{\text{Covariance}_k}{S_y S_y} = \frac{\sum_{t=1}^{n-k} (y_t - \bar{y})(y_{t+k} - \bar{y})}{\sum_{t=1}^n (y_t - \bar{y})^2} \quad (11)$$

where y is the sample, n is the sample size and S_y the standard deviation of the sample (Matematikcentrum 2012).

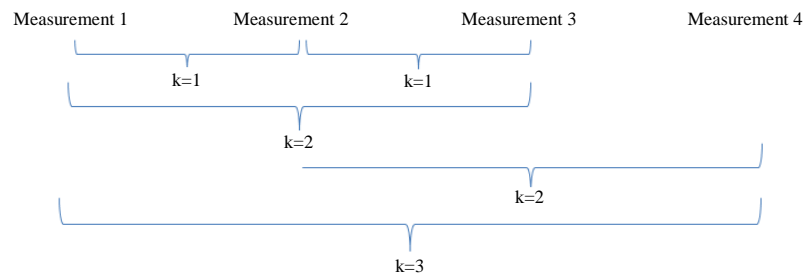


Figure 6: Describes the theory of lags and how they are used, where k is the lag distance.

The easiest way to describe the result is by plotting ρ for all lags (k) and illustrate the boundaries $(0 - \lambda_{0.025} \frac{1}{\sqrt{n}}, 0 + \lambda_{0.025} \frac{1}{\sqrt{n}})$ where ρ_k deviates significantly from zero outside the critical value of $\lambda_{0.025}$ (Matematikcentrum 2012).

3.4.4 Spearman ranked correlation

A third test, Spearman ranked correlations (Spearman 1904) was used to study the covariance over years between smoothed GCC and NDVI (Hufkens et al. 2012). While the Pearson correlation coefficient measures the linear relationship between two variables, the Spearman calculates the covariance of two measurements in segments and provides a correlation coefficient $(-1 < r_s < 1)$ for the dependence (Spearman 1904). In this way it was compared if GCC tends to grow, when NDVI increases. This was calculated with a similar principal as the autocorrelation through:

$$r_s = 1 - \frac{6 \cdot \sum_{i=1}^n (R_i - S_i)^2}{n^3 - n} \quad (12)$$

where R_i represents the replaced rank-value of GCC_i among the other GCC values, S_i represents the replaced rank-value of $NDVI_i$ among the other NDVI values and r_s is the rank-order correlation coefficient (Press et al. 1992). For the above equation 12 to work it is mandatory that tied ranks within the GCC and NDVI gets a suitable middle-rank (a rank that

is not an integer). When replacing the original data values with its corresponding rank value the test gets non-parametric properties. This is useful because of the fact that it does not matter if the variables are normally distributed or not (Press et al. 1992).

As well as with the other statistical methods, equation 10 is used to test if r_s deviates significantly ($P < 0.01$) from zero (Press et al. 1992).

All of the statistical calculations above were executed in MATLAB (R2013a; Mathworks, Natick, Massachusetts, USA).

4. RESULTS

4.1 Time Series

The measured and calculated GCC data from Norunda clear-cut show a strong seasonality. Figure 7 shows the smoothed GCC data reduced from 1712 to 200 data points through a 3-day running mean. Coefficient of determination (R^2) was calculated through a fitted 2nd-order polynomial regression for each year and ranges between 0.69 and 0.77. Interpolation was performed on the post-peak 2013 values (1st July - 1st August) as described in the methodology. Although there was a positive trend in GCC growth from 2011 to 2012, there seems to be stagnation between the peaks of 2012 and 2013 (Figure 7).

NDVI measurements (Figure 8) illustrate a similar seasonality and increasing trend as GCC (Figure 7). The NDVI also increases the first two years and slows down between 2012 and 2013. Coefficient of determination (R^2) was calculated for each year through a fitted 2nd-order polynomial regression and ranges between 0.49 and 0.68. Winter months were included. Both time series were plotted with two y-axes in figure 9 which aims at illustrating the covariance between the two data sets. Some differences were easy to see already at this stage, such as autumn 2012 which will be further analyzed in the next section.

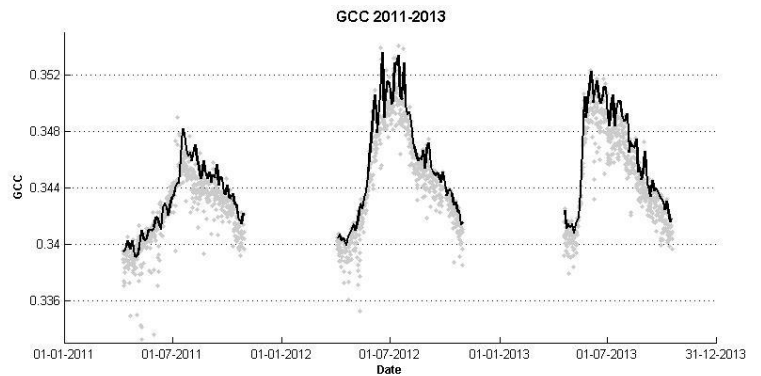


Figure 7: Measured GCC (Gray dots) and 3-day smoothed GCC (Black line) at Norunda clear-cut between April and October from 2011 to 2013.

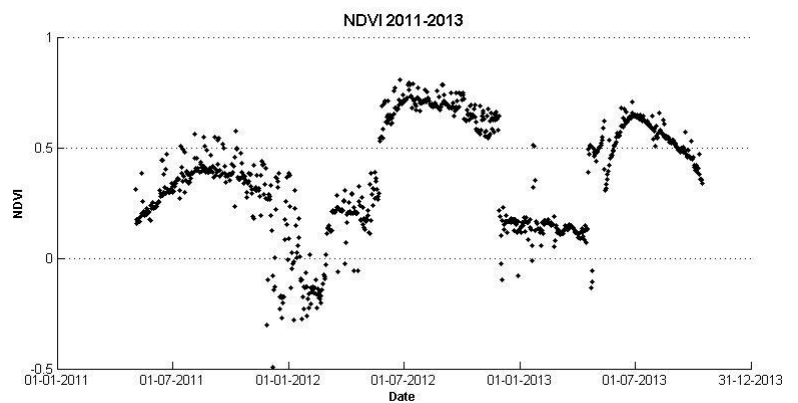


Figure 8: Measured and calculated NDVI (Normalized Difference Vegetation Index) from the SKYE 2-channel sensor at Norunda clear-cut with continuous data from 2011-2013.

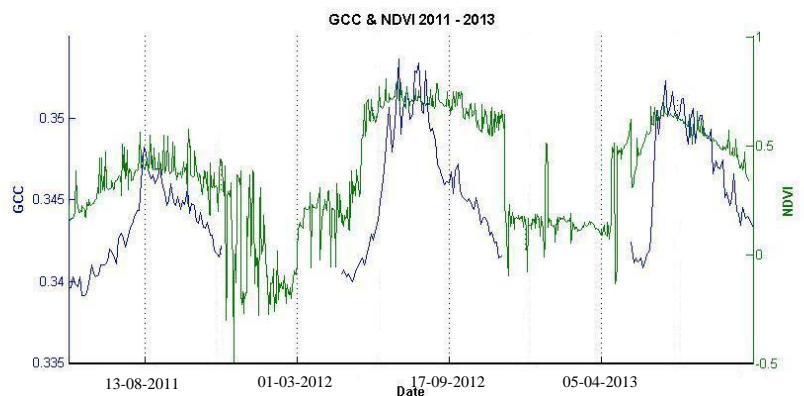


Figure 9: Smoothed GCC (Blue line) and NDVI (Green line) for 2011-2013 plotted together to see how the two time series covariate.

4.2 Statistics

4.2.1 GCC-NDVI comparison

The statistical test result of the smoothed GCC and the NDVI data (Figure 10a) shows a significant ($P < 0.01$) correlation ($r = 0.71$) which proves that GCC and NDVI measurements are related. The coefficient of determination is quite weak ($R^2 = 0.499$) which indicates a deviation in the linear dependence. This is easier to see in the correlation between the unsmoothed GCC and NDVI where the deviation is highlighted through circles in figure 10. Points inside the yellow circle (figure 10a, b) almost entirely represent dates during autumn, which means that GCC is retracting faster than NDVI during post-peak of growing season. As such the red circle contains points derived from spring measurements, which shows a faster increase in GCC than NDVI during vegetation growth in late spring. These irregularities can also be studied by the individual correlation for each year in figure 10 c, d and e. When looking at the yellow circle (Figure 10b) it is clear that the major part of its points consists of 2012 values, as with the red circle that holds similarities to 2013 points. However, data from all years are included in the different circles although it is important to highlight this unseasonal relation.

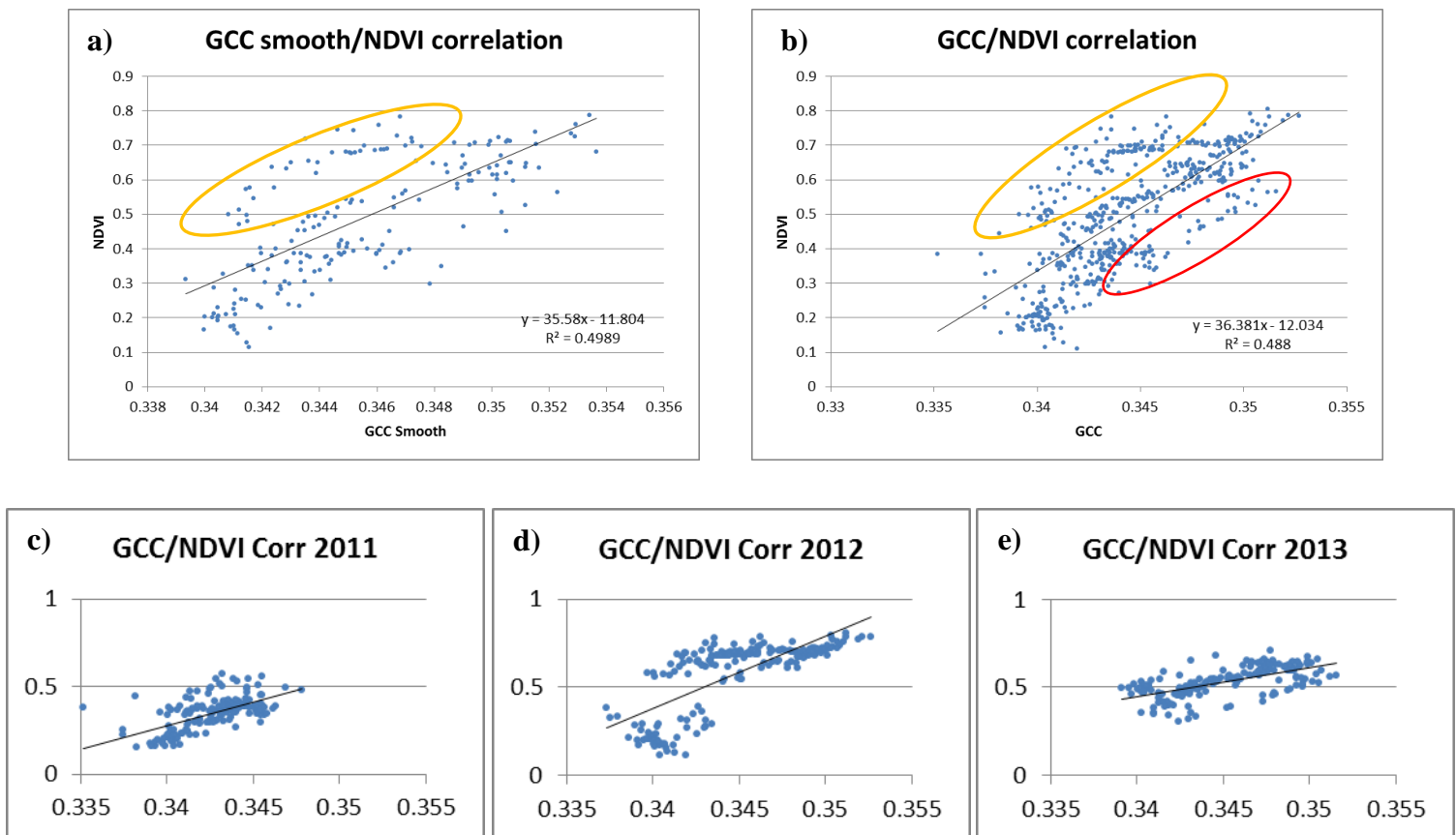


Figure 10: a) Correlation of smoothed GCC and NDVI where Pearson correlation coefficient is $r = 0.71$ ($P < 0.01$). b) Correlation of GCC and NDVI where Pearson correlation coefficient is $r = 0.70$ ($P < 0.01$). Circles highlights data points where GCC and NDVI are weakly correlated. Yellow circle represents data points where NDVI is higher and red circle represents data points where NDVI is lower. c), d) and e) show the correlation of unsmoothed GCC and NDVI for each year.

4.2.2 Autocorrelation and Spearman

The calculated autocorrelation shows a significant ($P < 0.05$) correlation between lags outside the $-0.14 < y < 0.14$ interval for the smoothed GCC and lags outside the $-0.066 < y < 0.066$ interval for the NDVI. The significant lags can be studied in figure 11 where a significant correlation occurs during the first 15 lags ($k=15$; Figure 6) for the smoothed GCC and 90 lags ($k=90$) for the NDVI. The decaying sinusoidal curve in both plots indicates that seasonality is represented in the time series. The decaying trend is normal where an autocorrelation always peaks at the origin. Negative correlation does also occur at some lags (Figure 11), these are often lag distances that represent the period from summer to autumn.

The spearman test gives a significant ($P < 0.01$) ranked correlation coefficient of 0.7206 which is slightly above the Pearson correlation result. No plot is shown because the spearman correlation is identical to the graphs above in the 4.2.1 section.

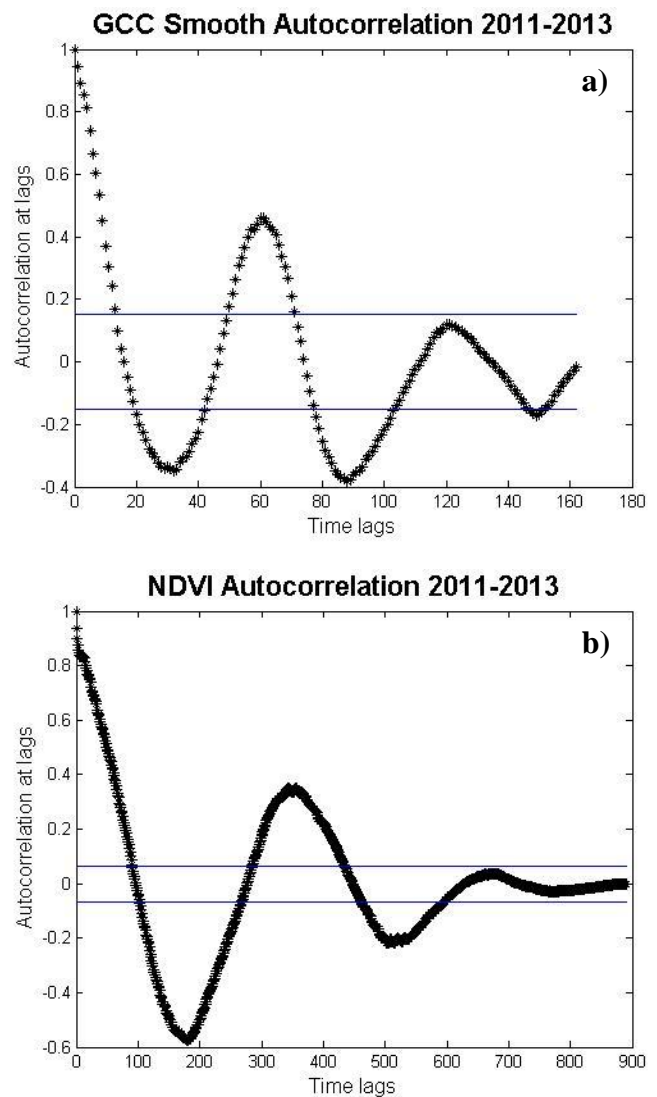


Figure 11: Calculated autocorrelation for smoothed GCC (a) and NDVI (b) data between 2011-2013. Number of lags is equal to number of data points (figure 6 & 7). There is a significant ($P < 0.05$) correlation at lag lengths located outside the blue lines.

4.3 Illumination calibration

The reference panels were studied as described in the Methodology section above. The white reference panel was evaluated by examining the occurrence of oversaturation in the 2012 camera pictures. The results show a large portion of oversaturation as seen in Figure 12a where 98 out of 598 (16 %) measurements hit the maximum value ($\overline{RGB} = 255$). This makes the white reference panel unusable for brightness calibration. However, the black reference panel is not able to get oversaturated which would make it the better contender for brightness calibration. As described in the Methodology section a Reference Index (RI) is calculated through equation 7 and plotted in figure 12b for the black reference panel during 2012. These values are applied to equation 8 to calculate the Calibrated GCC. The Coefficient of determination of the reference values (Figure 12b) and the calibrated GCC (Figure 12c) is calculated through a fitted 2nd-order polynomial regression (black line in both figures) where $R^2_{RI} \approx 0.35$ and $R^2_{Cal.GCC} \approx 0.58$. Compared to the original GCC values seen in figure 12c the R^2 -value of the calibrated GCC is substantially lower which indicates on a scattering effect of the brightness calibration.

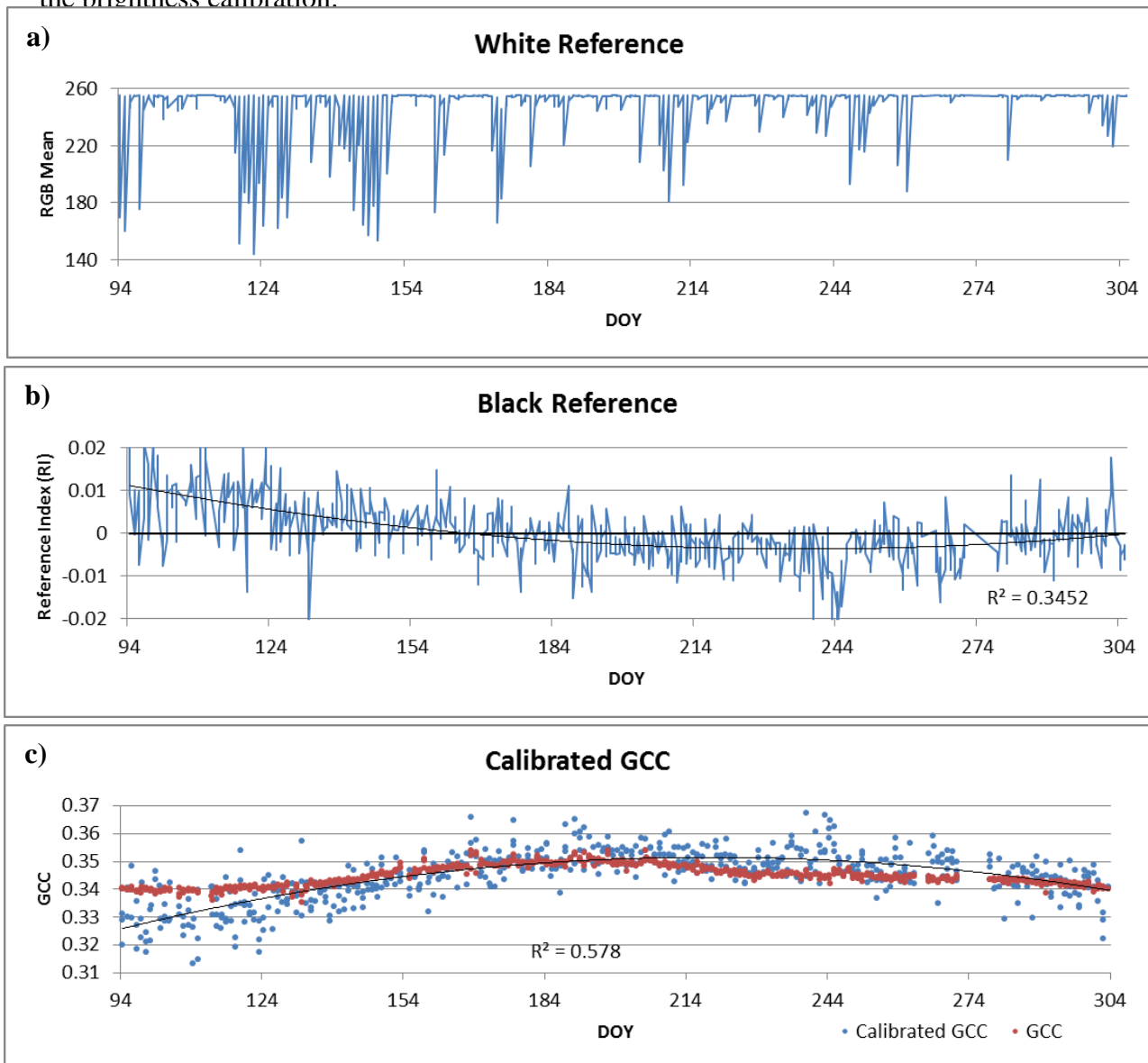


Figure 12: a) RGB mean per Day of Year (DOY) measured with a ROI_{ref} defined for the white reference panel (Figure 4). b) Brightness Index measured with a ROI_{ref} defined on the black reference panel (Figure 4). A fitted trend shows a concave seasonal relationship. c) Calibrated GCC values for 2012 (Blue Dots) through equation 8 with fitted 2nd-order polynomial regression line, compared to the uncalibrated 2012 GCC values (red dots).

5. DISCUSSION

5.1 Relationship between GCC and NDVI

As seen in the statistical results there is a significant correlation between GCC and NDVI measurements. Individually, the measurements show a significant seasonality seen in the autocorrelation in figure 11, which confirms that there is time-dependence. When compared, the two time series show similar patterns throughout the years (Figure 9), which is confirmed by the significant results given through calculations of linear correlation and spearman ranked correlation. These results indicate a strong similarity in precision and reliability between digital repeat photography and NDVI. The spearman test also confirms that the covariance is not random but actually follows through the time series, during the different seasons. However, as seen in figure 9 there are some differences between GCC and NDVI that explains why the correlation is not as strong as one would want it to be. The following paragraph will discuss the probable reasons and effects of these differences.

When studying the covariance between GCC and NDVI in figure 9 there is a clear difference in time series periodicity. It is easy to spot that the vegetation season is much shorter according to GCC measurements than NDVI. The difference also appears when studying the values that deviate from the linear dependence in figure 10a and b, and how these are exclusively situated during autumn. The explanation probably lies in the perception of the sensors where the NDVI sensor “sees” vegetation even if the green chlorophyll is absent, which is not the case with the digital camera. The spring values inside the red circle in figure 10b are not as easily explained and seem to be a phenomenon exclusively for 2013 when studying figures 10 c, d and e. Also the trend is not as easily compared to figure 9 which more or less show a similar spring covariance between GCC and NDVI. As such the measurements during autumn get different to NDVI which may indicate that the GCC method is more sensitive to variance in chlorophyll presence. Migliavacca et al. (2011) made a similar finding when studying a period of strong variation of drought and moist. Here, the digital repeat photography was still able to deliver reliable data due to the sensitivity of weekly variations. However, important information can be lost during periods such as autumn, information that the NDVI sensor still can supply.

Another similarity between GCC and NDVI measurements is the stagnation in growth from 2012 to 2013 where both indexes show how the progress levels off. When pictures from the same date, from different years get interpreted by a human, it is clear that a significant growth has occurred. This is probably an indication that vegetation of this kind does not reflect more green or infrared radiation than a certain level ($GCC \approx 0.355$; $NDVI \approx 0.8$). This suggests that even if the vegetation gets denser, it does not show in the measurements i.e. the surface is covered with vegetation in the two-dimensional footprint. If this is the case, this level is reached in 2012 and onwards which is seen in figure 7 and 8.

As a last note the measured NDVI-levels are very high for a grassland area ($NDVI \approx 0.8$). Values between 0.2 and 0.5 are usually the case (Weier and Herring 2000), which indicates an interesting relation. Maybe the ground of the clear-cut still contains a lot of vegetation that is not possible to see in the camera pictures, like mosses. However, these NDVI-values will probably decrease once the spruce starts to dominate the area. An interesting relation that is possible to study within the next five to ten years with the Norunda data.

5.2 Scene Illumination

The constant variation of incoming solar radiation is naturally the most influential variable when it comes to visible light sensing. While there are many methods to normalize these unwanted fluctuations this thesis has followed the theories of Sonnentag et al. (2012) and Hufkens et al. (2012). In figure 7 the diurnal variation is to a greater extent suppressed because of the use of chromatic coordinates and the 3-day smoothing. Compared to the NDVI measurements (Figure 8), the smoothed GCC suffers from a significantly lower diurnal variation, even if the NDVI sensor is more carefully calibrated.

5.2.1 Reference panels

The results from the reference panels follows the findings of Sonnentag et al. (2012), where problems such as strong variation and oversaturation do more harm than good. The major problem with the reference panels used for this thesis is the choice of colors and location. First, the use of black, but primarily white color is unfortunately unusable due to the oversaturation seen in figure 12a. To put it simple the digital camera gets blinded by the high reflectance of the white color on a sunny day. The panel gets similar properties of a mirror where the camera determines the measurement to the highest possible value. On the other hand the use of black color is risky but seems to be sufficient enough in this case (Figure 12b). Secondly, the strong variance of the GCC_{ref} makes it unwise to implement the calibration into the analysis. When studying the calibrated GCC (figure 12c) the variance has been imported and thus made the trend less reliable. This strong variance of the GCC_{ref} is probably caused by the size or placement of the reference panel (Figure 4). Here it would have been better to follow the principle of Ahrends et al. (2008); Richardson et al. (2009) and Migliavacca et al. (2011) where a closer located panel, mounted just in front of the camera, would be preferable. Although there are advantages with reference panels placed on the ground such as a more representable measurement of brightness at vegetation level. Maybe the reference panel should just have been larger in size. However, both of the above methods results in a reference panel covering a larger part of the picture, hence it is important to place it strategically, not covering an area of interest.

In the Norunda pictures the reference panel only covers a small number of pixels which leads to weak calculations of the brightness mean. This corrupts the credibility of the GCC_{ref} because of the risk of randomness and thus a strong variation. Another disadvantage with the size of the panels is the extra-long peaks seen in figure 12a and b. These are probably caused by the wind tilting the tower and thus placing the ROI_{ref} outside the reference panels. This leads to reference-measurements containing vegetation, which gives a higher or lower GCC_{ref} depending on the color of the panel. As mentioned earlier this would not had been a problem if the reference panels covered a greater amount of pixels or if it was mounted on the tower in front of the camera. However, there is another workaround where the ROI_{ref} is not defined in pixel coordinates, as it currently is, but in picture elements. This would need a picture analysis script that identifies the reference panel and defines a ROI_{ref} within each picture. A quite complicated method that was not possible to include in this thesis.

In figure 12b there is a concave trend in the reference index during the 2012 vegetation season. It is hard to tell the reason when the hemispherical irradiance, measured parallel to NDVI (Equation 4), holds a distinct convex trend. The result however, is that the RI has a detrending effect when used as a calibration on GCC measurements which is another disadvantage with the reference panels. As with the studies of Ahrends et al. (2008) and Sonnentag et al. (2012) the use of reference panels are inaccurate and can possible do more harm than good.

5.3 Applicability

5.3.1 Scientific

The use of digital repeat photography is primarily relevant for the scientific sector. Earlier research has mainly focused on measuring phenology patterns to see the effects of climate change on plant growing cycle (Richardson et al. 2009). As mentioned in the introduction the phenology research was, prior to Richardson et al. (2007), carried out through field observations and satellite remote sensing. However, the work since has revolved around a rather successful implementation of digital repeat photography. As proven through this thesis, the method is also useful when following vegetation development on clear-cut areas. It has been shown that the flora regrowth of a clear-cut has a large impact on the emissions of stored carbon in the soil (Nakane and Lee 1995). According to Nakane and Lee (1995) it takes about 40 – 50 years for the soil to recover the lost carbon after clear-cutting, where the most crucial period of CO₂-emission rate is immediately after logging. Every year approximately 200 000 hectares of forest is felled in Sweden (Skogsstyrelsen 2013) which makes the scientific work valuable for climate research. Maybe it is possible to study different crops to cultivate clear-cut areas and thus find an appropriate way to lower the amount of evaporating soil carbon. A method such as the digital repeat photography can be important for future scientific progress because of its unique mixture of sensor-based measurements and field observations.

5.3.2 Industrial

Digital repeat photography is a good method that can be used, not only in the scientific sector, but also in the forest industry. As shown by Ahrends et al. (2009) and Richardson et al. (2009) the greenness analysis is well correlated with GPP and NEE measurements which could be used to develop an overall forest analysis tool. However, before this is a reliable method extensive research must be performed. When using linked dependencies it is important that the model is calibrated to the studied climate and forest type, and not imported from somewhere else. Therefore the author of this thesis recommends further study of narrow regressions limited to different forest types and climatic regions. By simplifying the management and making the analysis more accessible, the forest farmer can monitor the growth from clear-cut to full grown trees with an inexpensive tool. According to Sonesson (, Personal communications, 2014) the implementation of digital methods in the forestry sector is still on a scientific level. The goal is to give the farmer new tools to help determine the right time for thinning, final cutting and other forestry processes (Sonesson, Personal communications, 2014). The main reason to the missing industry implementation is primarily the use of expensive tools such as laser scanners. These are not economically sustainable for forest farmer and therefore only used by the research sector (Sonesson, Personal communications, 2014). However, as shown in this thesis the digital cameras are reliable and affordable, and could potentially be a useful tool in a modernized forest industry.

5.3.3 Future research

As mentioned above, the digital repeat photography method still needs additional research and uncertainty analysis to be fully reliable and useful. Further studies like the work of this thesis, linking the clear-cut GCC to CO₂ flux data or satellite NDVI, is needed for the method to be applicable to the different practices discussed above. Also, the need of a technical protocol discussed by Ide and Oguma (2010) is necessary for further research and the possibility to apply the method on a larger scale.

Using digital repeat photography for monitoring the regrowth of a clear-cut area

6. CONCLUSION

The work of this thesis has revolved around analyzing digital images and NDVI data from the Norunda clear-cut in central Sweden. The two methods have been compared in order to determine whether the digital repeat photography is an equally reliable and precise method as the sensor-based NDVI measurements. The assembled results show significant similarities between the two methods when monitoring the regrowth of the sparse vegetation. However, some deviations between the methods are found, primarily during the autumn senescence.

The benefit of this finding is the possibility to monitor forest ecology in a continuous way from the initial cultivation to logging, where this thesis complements earlier research that mainly focused on adult trees and phenology. A further analysis of digital cameras and clear-cut areas is possible through the study of connections between the initial stage of regrowth and soil carbon release. Another application, on a more long-term-level, is the implementation in the forestry industry where the method would give farmers a tool to evaluate different stages in the forest cultivation process. It is, however, recommended that further research is applied to calibrate the method for measurements in different forest types and climate zones.

In this thesis the difficulties, and different methods, to suppress scene illumination has also been studied. Ground-level reference panels have been analyzed and shown to be unreliable with too many sources of error. Instead, chromatic coordinates have been used as suggested by earlier research that proves the low influence of diurnal and seasonal changes in scene illumination.

REFERENCES

- Ahrends, H. E., R. Brugger, R. Stockli, J. Schenk, P. Michna, F. Jeanneret, H. Wanner, and W. Eugster. 2008. Quantitative phenological observations of a mixed beech forest in northern Switzerland with digital photography. *Journal of Geophysical Research-Biogeosciences*, 113: 11. DOI: 10.1029/2007jg000650
- Ahrends, H. E., S. Etzold, W. L. Kutsch, R. Stoeckli, R. Bruegger, F. Jeanneret, H. Wanner, N. Buchmann, et al. 2009. Tree phenology and carbon dioxide fluxes: use of digital photography at for process-based interpretation the ecosystem scale. *Climate Research*, 39: 261-274. DOI: 10.3354/cr00811
- Eklundh, L., H. X. Jin, P. Schubert, R. Guzinski, and M. Heliasz. 2011. An Optical Sensor Network for Vegetation Phenology Monitoring and Satellite Data Calibration. *Sensors*, 11: 7678-7709. DOI: 10.3390/s110807678
- Hufkens, K. 2010. PhenoCam GUI. Retrieved 2-12 2013, from <http://phenocam.sr.unh.edu/webcam/tools/>
- Hufkens, K., M. Friedl, O. Sonnentag, B. H. Braswell, T. Milliman, and A. D. Richardson. 2012. Linking near-surface and satellite remote sensing measurements of deciduous broadleaf forest phenology. *Remote Sensing of Environment*, 117: 307-321. DOI: <http://dx.doi.org/10.1016/j.rse.2011.10.006>
- Ide, R., and H. Oguma. 2010. Use of digital cameras for phenological observations. *Ecological Informatics*, 5: 339-347. DOI: 10.1016/j.ecoinf.2010.07.002
- Jin, H. Personal communications, 2013. Transformation of RVI to NDVI. ed. L. Forslund.
- Lillesand, M. T., W. R. Kiefer, and W. J. Chipman. 2008. *Remote sensing and image interpretation*. Hoboken, NJ, USA: John Wiley & Sons.
- Lundin, L. C., S. Halldin, A. Lindroth, E. Cienciala, A. Grelle, P. Hjelm, E. Kellner, A. Lundberg, et al. 1999. Continuous long-term measurements of soil-plant-atmosphere variables at a forest site. *Agricultural and Forest Meteorology*, 98-9: 53-73. DOI: 10.1016/s0168-1923(99)00092-1
- Matematikcentrum. 2012. SAMBANDSANALYS: Regression och Korrelation, Orientering om Tidsserier. 44 pp. Matematisk Statistik, Matematikcentrum, LTH, Lunds Universitet
- Migliavacca, M., M. Galvagno, E. Cremonese, M. Rossini, M. Meroni, O. Sonnentag, S. Cogliati, G. Manca, et al. 2011. Using digital repeat photography and eddy covariance data to model grassland phenology and photosynthetic CO₂ uptake. *Agricultural and Forest Meteorology*, 151: 1325-1337. DOI: <http://dx.doi.org/10.1016/j.agrformet.2011.05.012>
- Morisette, J. T., A. D. Richardson, A. K. Knapp, J. I. Fisher, E. A. Graham, J. Abatzoglou, B. E. Wilson, D. D. Breshears, et al. 2009. Tracking the rhythm of the seasons in the face of global change: phenological research in the 21st century. *Frontiers in Ecology and the Environment*, 7: 253-260. DOI: 10.1890/070217
- Nakane, K., and N. J. Lee. 1995. Simulation of soil carbon cycling and carbon balance following clear-cutting in a mid-temperate forest and contribution to the sink of atmospheric CO₂. *Vegetatio*, 121: 147-156. DOI: 10.1007/bf00044680
- Press, W. H., B. P. Flannery, S. A. Teukolsky, and W. T. Vetterling. 1992. Nonparametric or Rank Correlation. In *Numerical Recipes in C: The Art of Scientific Computing: Second Edition*, 639-642 pp. Cambridge: Cambridge University Press.
- Richardson, A. D., B. H. Braswell, D. Y. Hollinger, J. P. Jenkins, and S. V. Ollinger. 2009. Near-surface remote sensing of spatial and temporal variation in canopy phenology. *Ecological Applications*, 19: 1417-1428. DOI: 10.1890/08-2022.1

- Richardson, A. D., J. P. Jenkins, B. H. Braswell, D. Y. Hollinger, S. V. Ollinger, and M. L. Smith. 2007. Use of digital webcam images to track spring green-up in a deciduous broadleaf forest. *Oecologia*, 152: 323-334. DOI: 10.1007/s00442-006-0657-z
- Skogsstyrelsen. 2013. Felling and Wood Measurement. In Swedish Statistical Yearbook of Forestry 2013. 151-171. www.skogsstyrelsen.se.
- Sonesson, J., Personal communications, 2014. Questions to the Head of "The digital forest" at skogsforsk.se: The implementation of digital methods in forest research and industry. ed. L. Forslund.
- Sonnentag, O., K. Hufkens, C. Teshera-Sterne, A. M. Young, M. Friedl, B. H. Braswell, T. Milliman, J. O'Keefe, et al. 2012. Digital repeat photography for phenological research in forest ecosystems. *Agricultural and Forest Meteorology*, 152: 159-177. DOI: <http://dx.doi.org/10.1016/j.agrformet.2011.09.009>
- Spearman, C. 1904. The proof and measurement of association between two things. *American Journal of Psychology*, 15: 72-101. DOI: 10.2307/1412159
- Weier, J., and D. Herring. 2000. Measuring Vegetation (NDVI & EVI). Retrieved 10-12 2013, from <http://earthobservatory.nasa.gov/Features/MeasuringVegetation/>
- Zhao, J., Y. Zhang, Z. Tan, Q. Song, N. Liang, L. Yu, and J. Zhao. 2012. Using digital cameras for comparative phenological monitoring in an evergreen broad-leaved forest and a seasonal rain forest. *Ecological Informatics*, 10: 65-72. DOI: <http://dx.doi.org/10.1016/j.ecoinf.2012.03.001>

Institutionen för naturgeografi och ekosystemvetenskap, Lunds Universitet.

Student examensarbete (Seminarieuppsatser). Uppsatserna finns tillgängliga på institutionens geobibliotek, Sölvegatan 12, 223 62 LUND. Serien startade 1985. Hela listan och själva uppsatserna är även tillgängliga på LUP student papers (www.nateko.lu.se/masterthesis) och via Geobiblioteket (www.geobib.lu.se)

The student thesis reports are available at the Geo-Library, Department of Physical Geography and Ecosystem Science, University of Lund, Sölvegatan 12, S-223 62 Lund, Sweden. Report series started 1985. The complete list and electronic versions are also electronic available at the LUP student papers (www.nateko.lu.se/masterthesis) and through the Geo-library (www.geobib.lu.se)

- 245 Linnea Jonsson (2012). Impacts of climate change on Pedunculate oak and Phytophthora activity in north and central Europe
- 246 Ulrika Belsing (2012) Arktis och Antarktis föränderliga havsistäcken
- 247 Anna Lindstein (2012) Riskområden för erosion och näringsläckage i Segeåns avrinningsområde
- 248 Bodil Englund (2012) Klimatanpassningsarbete kring stigande havsnivåer i Kalmar läns kustkommuner
- 249 Alexandra Dicander (2012) GIS-baserad översvämningsskartering i Segeåns avrinningsområde
- 250 Johannes Jonsson (2012) Defining phenology events with digital repeat photography
- 251 Joel Lilljebjörn (2012) Flygbildsbaserad skyddszonsinventering vid Segeå
- 252 Camilla Persson (2012) Beräkning av glaciärers massbalans – En metodanalys med fjärranalys och jämviktlinjehöjd över Storglaciären
- 253 Rebecka Nilsson (2012) Torkan i Australien 2002-2010 Analys av möjliga orsaker och effekter
- 254 Ning Zhang (2012) Automated plane detection and extraction from airborne laser scanning data of dense urban areas
- 255 Bawar Tahir (2012) Comparison of the water balance of two forest stands using the BROOK90 model
- 256 Shubhangi Lamba (2012) Estimating contemporary methane emissions from tropical wetlands using multiple modelling approaches
- 257 Mohammed S. Alwesabi (2012) MODIS NDVI satellite data for assessing drought in Somalia during the period 2000-2011
- 258 Christine Walsh (2012) Aerosol light absorption measurement techniques: A comparison of methods from field data and laboratory experimentation

- 259 Jole Forsmoo (2012) Desertification in China, causes and preventive actions in modern time
- 260 Min Wang (2012) Seasonal and inter-annual variability of soil respiration at Skyttorp, a Swedish boreal forest
- 261 Erica Perming (2012) Nitrogen Footprint vs. Life Cycle Impact Assessment methods – A comparison of the methods in a case study.
- 262 Sarah Loudin (2012) The response of European forests to the change in summer temperatures: a comparison between normal and warm years, from 1996 to 2006

- 263 Peng Wang (2012) Web-based public participation GIS application – a case study on flood emergency management
- 264 Minyi Pan (2012) Uncertainty and Sensitivity Analysis in Soil Strata Model Generation for Ground Settlement Risk Evaluation
- 265 Mohamed Ahmed (2012) Significance of soil moisture on vegetation greenness in the African Sahel from 1982 to 2008
- 266 Iurii Shendryk (2013) Integration of LiDAR data and satellite imagery for biomass estimation in conifer-dominated forest
- 267 Kristian Morin (2013) Mapping moth induced birch forest damage in northern Sweden, with MODIS satellite data
- 268 Ylva Persson (2013) Refining fuel loads in LPJ-GUESS-SPITFIRE for wet-dry areas - with an emphasis on Kruger National Park in South Africa
- 269 Md. Ahsan Mozaffar (2013) Biogenic volatile organic compound emissions from Willow trees
- 270 Lingrui Qi (2013) Urban land expansion model based on SLEUTH, a case study in Dongguan City, China
- 271 Hasan Mohammed Hameed (2013) Water harvesting in Erbil Governorate, Kurdistan region, Iraq - Detection of suitable sites by using Geographic Information System and Remote Sensing
- 272 Fredrik Alström (2013) Effekter av en havsnivåhöjning kring Falsterbohalvön.
- 273 Lovisa Dahlquist (2013) Miljöeffekter av jordbruksinvesteringar i Etiopien
- 274 Sebastian Andersson Hylander (2013) Ekosystemtjänster i svenska agroforestrysystem
- 275 Vlad Pirvulescu (2013) Application of the eddy-covariance method under the canopy at a boreal forest site in central Sweden
- 276 Malin Broberg (2013) Emissions of biogenic volatile organic compounds in a Salix biofuel plantation – field study in Grästorp (Sweden)
- 277 Linn Renström (2013) Flygbildsbaserad förändringsstudie inom skyddszoner längs vattendrag
- 278 Josefin Methi Sundell (2013) Skötsel effekter av miljöersättningen för natur- och kulturmiljöer i odlingslandskapets småbiotoper
- 279 Kristín Agustsdóttir (2013) Fishing from Space: Mackerel fishing in Icelandic waters and correlation with satellite variables
- 280 Cristián Escobar Avaria (2013) Simulating current regional pattern and composition of Chilean native forests using a dynamic ecosystem model
- 281 Martin Nilsson (2013) Comparison of MODIS-Algorithms for Estimating Gross Primary Production from Satellite Data in semi-arid Africa
- 282 Victor Strevens Bolmgren (2013) The Road to Happiness – A Spatial Study of Accessibility and Well-Being in Hambantota, Sri Lanka
- 283 Amelie Lindgren (2013) Spatiotemporal variations of net methane emissions and its causes across an ombrotrophic peatland - A site study from Southern Sweden
- 284 Elisabeth Vogel (2013) The temporal and spatial variability of soil respiration in boreal forests - A case study of Norunda forest, Central Sweden
- 285 Cansu Karsili (2013) Calculation of past and present water availability in the Mediterranean region and future estimates according to the Thornthwaite water-balance model
- 286 Elise Palm (2013) Finding a method for simplified biomass measurements on Sahelian grasslands
- 287 Manon Marcon (2013) Analysis of biodiversity spatial patterns across multiple

- taxa, in Sweden
- 288 Emma Li Johansson (2013) A multi-scale analysis of biofuel-related land acquisitions in Tanzania - with focus on Sweden as an investor
- 289 Dipa Paul Chowdhury (2013) Centennial and Millennial climate-carbon cycle feedback analysis for future anthropogenic climate change
- 290 Zhiyong Qi (2013) Geovisualization using HTML5 - A case study to improve animations of historical geographic data
- 291 Boyi Jiang (2013) GIS-based time series study of soil erosion risk using the Revised Universal Soil Loss Equation (RUSLE) model in a micro-catchment on Mount Elgon, Uganda
- 292 Sabina Berntsson & Josefin Winberg (2013) The influence of water availability on land cover and tree functionality in a small-holder farming system. A minor field study in Trans Nzoia County, NW Kenya
- 293 Camilla Blixt (2013) Vattenkvalitet - En fältstudie av skånska Säbybäcken
- 294 Mattias Spångmyr (2014) Development of an Open-Source Mobile Application for Emergency Data Collection
- 295 Hammad Javid (2013) Snowmelt and Runoff Assessment of Talas River Basin Using Remote Sensing Approach
- 296 Kirstine Skov (2014) Spatiotemporal variability in methane emission from an Arctic fen over a growing season – dynamics and driving factors
- 297 Sandra Persson (2014) Estimating leaf area index from satellite data in deciduous forests of southern Sweden